ARID ZONE JOURNAL OF ENGINEERING, TECHNOLOGY & ENVIRONMENT
AZOJETE September 2023. Vol. 19(3):519-536
Published by the Faculty of Engineering, University of Maiduguri, Maiduguri, Nigeria.
Print ISSN: 1596-2490, Electronic ISSN: 2545-5818
www.azojete.com.ng

ORIGINAL RESEARCH ARTICLE

EVALUATION AND COMPARISON OF SOME INFILTRATION MODELS ON AGRICULTURAL SOILS OF BOSSO LOCAL GOVERNMENT AREA, NIGER STATE, NIGERIA

J. J. Musa[1]*, I. A. Kuti[1], P. O. O. Dada[2], E. A. Otuaro[3], P. C. Eze[4], and S. O. Nathaniel[1]

[1]Department of Agricultural and Bioresources Engineering, Federal University of Technology, P. M. B. 65, Minna, Nigeria
[2]Department of Agricultural and Bioresources Engineering, Federal University of Agriculture, P. M. B. 102, Abeokuta, Nigeria
[3]Department of Civil Engineering, Nigeria Maritime University, Okerenkoko, Nigeria
[4]Department of Soil Science and Land Management, Federal University of Technology, P. M. B. 65, Minna, Nigeria.

**Corresponding author's email address: johnmusa@futminna.edu.ng*

ARTICLE INFORMATION

Submitted 16 June 2023
Revised 5 August, 2023
Accepted 10 August, 2023

Keywords:
Bosso
infiltration models
Kostiakov
Philip
Modified Kostiakov
US-Soil Conservation Service (SCS)

ABSTRACT

Over the last few decades, researchers have developed a great interest in fabricating and synthesising zinc silicate-based glass ceramics. However, using waste materials as precursors for the fabrication is yet another milestone in waste management. Thus, this study fabricated zinc silicate glass-ceramic using sola lime silica (SLS) glass waste as a silicon source. The series of precursor glass in the $(ZnO)_{0.6-x}\,(B_2O_3)_x\,(SLS)_{0.4}$ *the conventional solid-state melt-quench technique prepared system through a controlled crystallisation process. The glass system's physical, structural, and optical properties were obtained by density measurement, X-Ray diffraction, Fourier Transform Infrared Spectroscopy, and Ultraviolet-visible spectroscopy, respectively. The density of the* $(ZnO)_{0.6-x}\,(B_2O_3)_x\,(SLS)_{0.4}$ *glasses series was observed to be decreasing with the increment of* $wt.\%\,B_2O_3$ *content. The XRD spectra of the* $(ZnO)_{0.6-x}\,(B_2O_3)_x\,(SLS)_{0.4}$ *samples with 0 and 0.01 wt.%* B_2O_3*, exhibits major diffraction peaks attributed to the ZnO phase in the glass matrix. However, as* B_2O_3 *content increased, the precursor glass sample shown by the XRD spectra depicted a broad halo characteristic, which reflected the properties of amorphous glass that were observed at the composition of 0.05 wt.%* B_2*. From FTIR spectra, the bands at 500, 688, 902 and 1243* cm^{-1} *can be associated with stretching vibrations of* ZnO_4 *and Si-O-B bending vibrations, stretching vibrations of the B–O bonds in the* BO_4 *units, and modes of boron–oxygen triangular* BO_3 *units. The intensity of the IR band increases with increasing percentage of* B_2O_3*. The UV-Vis analysis of the samples with 0 and 0.01 wt.%* B_2O_3 *demonstrates crystalline hump and varies at 370 nm. It was observed that the addition of* B_2O_3 *to the ZnO-SLS glass network caused the glassy amorphous state without a sharp absorption edge at 0.05, 0.10, and 0.15 wt.%* B_2O3*.The* $(ZnO)_{0.6-x}\,(B_2O_3)_x\,(SLS)_{0.4}$ *system shows the increase in band gap when the composition of* B_2O_3 *increased. When* ZnO *serves as a modifier, the number of NBOs will increase, and this will cause the expansion of glass network. The zinc silicate-based glass-ceramic produced has been classified as a semiconductor due to the vast optical band gap energy obtained and may have vital potential applications for future LED and other optoelectronic lighting devices.*

1.0 Introduction

Soil compaction changes the physical properties of soil by increasing its strength and bulk density, lowering its porosity, and forcing a narrower pore size distribution within the soil. These changes

impact how air and water circulate through the soil, as well as the capacity of roots to develop in it (Sollins and Gregg, 2017; Jury and Stolzy, 2018, Lal *et al*., 2018). The infiltration rate can be affected by changes in how air and water travel through the soil. Higher runoff volume, increased flooding potential, and less groundwater recharge within watersheds resulting from a lower infiltration rate.

Infiltration is a critical technique in managing water resources for crop production in irrigated and dry agricultural environments. It is a precondition for constructing, analysing and managing irrigation systems. Similarly, knowledge of infiltration is required to model, critically evaluate, and design management solutions to conserve soil and water resources in dry-farming circumstances. Different variables can considerably impact the appropriate evaluation, modelling, and use of infiltration data. According to Barros *et al*. (2014), the activation of hydrological processes such as surface runoff, erosion, and solute transport is affected by undulations and spatial inhomogeneity of soil, spatial and temporal changes in soil use, and changes in soil water infiltration affected by climate change. Soil science, hydrology, irrigation, agriculture, civil engineering, environmental engineering and science rely on infiltration (Valiantzas, 2010) for irrigation. The hydrological modelling process requires an understanding of infiltration models. Along with occurrence time and runoff volume, infiltration regulates water division, water redistribution within soils, and even water-deep percolation down to groundwater. According to Angelaki *et al*. (2013), the infiltration rate is influenced by several factors, such as soil moisture level, texture, density, and behaviour.

Researchers have condensed soil infiltration features into various mathematical models (Musa and Egharevba, 2009; Al-Janobi *et al.*, 2010; Umar *et al*., 2021). However, model predictions must be proved by proper field verification, with the agreement between observed and anticipated values **(**Ogbe *et al*., 2011**).** Water infiltration into the soil can be monitored in the field or approximated using mathematical models that are either empirical or theoretically based on physical principles. Empirical models can relate model parameters to soil characteristics without requiring a physical meaning, which could include factors that are difficult to consider in theoretical models to determine their constants **(**Mirzaee *et al*., 2014).

Therefore, the study aims to determine the best model for the soil of built-up areas in Bosso-Campus of the Federal University of Technology, Minna, Niger State.

2.0 Materials and Methods

2.1 Description of the Study Area

The study area is located between Latitudes 9°39'3.82"N to 9°39'25.90 "N and Longitude 6°31'27.65 "E to 6°31'27.65 "E at an elevation of 400 m above sea level within Bosso Local Government Area of Niger State. The area's mean annual maximum and minimum temperatures are 39.18 °C and 25.86 °C, respectively, while the mean relative humidity and rainfall are 56.28 % and 130.0 mm, respectively. Bosso has two distinct central climates: rainy and dry seasons. The rainy season spans between April and October, while the dry season is between November and March.

Corresponding author's e-mail address: johnmusa@futminna.edu.ng

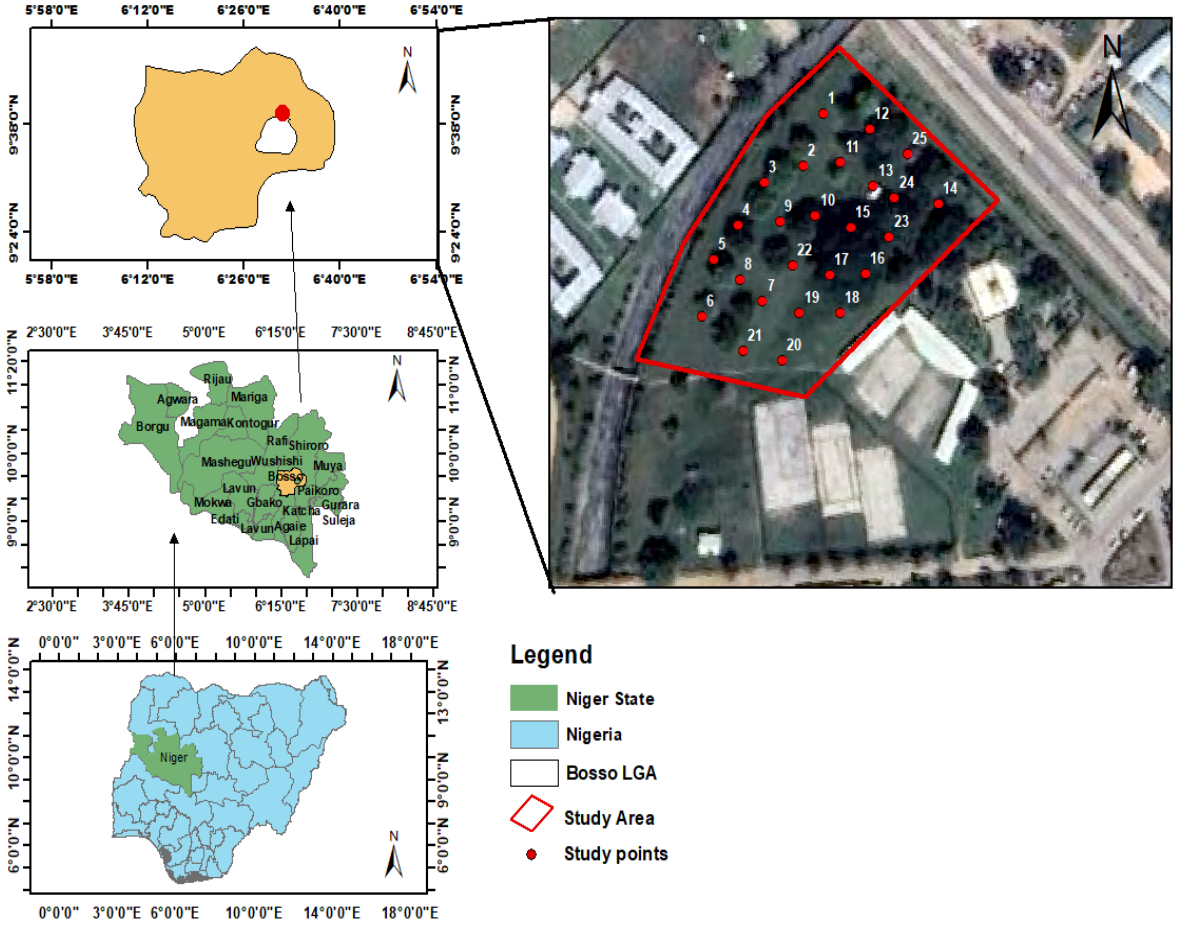

Figure 1: Map showing selected study area within Federal University of Technology Minna, Bosso Campus

2.2 Methodology

2.2.1 Soil sampling

A core sampler collected 15 soil samples from five selected locations at 0-30cm and 30 – 60cm depths. The soil samples were placed inside polythene bags and carefully labelled before being taken to the laboratory. These soil samples were analysed in the Soil and Water Laboratory of the Agricultural and Bioresources Engineering Department, Federal University of Technology, Minna. The soil properties tested include soil moisture content, bulk density, and soil texture (sand %, silt %, and clay %).

2.2.1.1 Determination of soil Moisture content

The soil samples collected from each sample point were oven-dried at 105^{0}C for 24 hours, and the moisture content was determined using Equation 1. This is in accordance with the work of Umaru *et al*. (2021).

$$MC\ (\%) = \frac{W_2 - W_3}{W_3 - W_1}\ X\ 100 \qquad (1)$$

Where Mc is the moisture content of the soil (%); W_1 is the weight of the container (g); W_2 is the weight of the container and sample before drying (g); and W_3 is the weight of the container and sample after oven drying (g).

2.2.1.2 Determination of soil bulk density

The bulk density was calculated using Equation 2 from the mass of oven-dried soil per core volume (g/cm^3).

$$\rho_b(gcm^{-3}) = \frac{Mass\ of\ oven\ dried\ soil\ (g)}{Volume\ of\ core\ sampler\ (cm^3)} \quad (2)$$

2.2.1.3 Particle size analysis

The hydrometer method determined the particle size distribution of the soil samples collected from the study area, which is in accordance with Panagos et al. (2014). The soil textural triangle was then used to determine the textural class of the soil samples.

2.3 Infiltration Rate Estimation Models and Parameters

The following infiltration models were considered for this study.

2.3.1 Philip Model

The infiltration model proposed by Philip includes the soil sorptivity (S) and stable infiltration rate (A) from the series of solutions from Richards' equation (Philip 1957). The two-term infiltration equation of Philip is expressed in Equations 3 and 4.

$$i_{(t)} = St^{1/2} + At \quad (3)$$

The differentiation of equation (1) yields equation 4 for infiltration rate (i).

$$i_{(t)} = \left(\frac{St^{-1/2}}{2}\right) + A \quad (4)$$

Where *i(t)* represents the infiltration rate and the cumulative infiltration at infiltration time (t), respectively, a is related to saturated hydraulic conductivity (K_{sat}), *S* is the soil water sorptivity term, and *t* is the time elapsed.

2.3.2 Kostiakov Model

Kostiakov proposed one of the earliest empirical infiltration models Hillel, (1982) for estimating the infiltration rate, as presented in equation 5 (Kostiakov 1932).

$$i_{(t)} = Kt^a \quad (5)$$

Where *I(t)* is the infiltration rate (mm min^{-1}) at time *t* (min), and a >0 (Kostiakov's time coefficient) and $0 < a < 1$. k and a are coefficients, the Kostiakov model parameters depend on the soil texture and conditions, including initial moisture content. The integration of equation 5 gives the expression of cumulative infiltration I (t) in mm, as presented in equation 6.

$$I_{(t)} = \left(\frac{K}{1-a}\right) t^{1-a} \quad (6)$$

Corresponding author's e-mail address: johnmusa@futminna.edu.ng

2.3.4. Modified Kostiakov model

The Kostiakov-Lewis or Menzencev model (equation 7) was developed to overcome the limitations of the initial Kostiakov equation (Sihag *et al*., 2017)**.**

$$i_t = Kt^a + f_0 t \quad (7)$$

2.3.5. US- Soil Conservation Service (SCS) model

The US Department of Agricultural, Natural Resources and Conservation Service summarised long-term experimental data as suggested in Kostiakov's model as complex. Therefore, a recommended coefficient of 0.6985 was added to the Kostiakov model to improve its performance and practical applicability as in equation 8.

$$i_t = at^b + 0.6985 \quad (8)$$

Where *i(t)* represents the cumulative infiltration

2.4 Statistical Analysis

The statistical indices used in evaluating the models' performance are presented in Equations 9 to 11.

2.4.1 Root Mean Square Error (RMSE)

The RMSE for the data obtained was determined using equation 9.

$$RMSE = \sqrt{\frac{1}{N}\sum_{i=1}^{N}(p_i - m_i)_i^2} \quad (9)$$

2.4.2 Coefficient of Determination (R^2)

The models' efficacy was assessed using the coefficient of determination presented in Equation 10.

$$R^2 = 1 - \frac{\sqrt{\sum_{i=1}^{N}(P_i - P)^{i2}}}{\sqrt{\sum_{i=1}^{n}(m_i - m)^{i2}}} \quad (10)$$

2.4.3 Coefficient of Correlation (CC)

The effectiveness of the numerical predictions of the infiltration models was evaluated using the correlation coefficient as presented in Equation 11.

$$CC = \frac{z\sum ab - \sum a - \sum b}{\sqrt{z(\sum a^2) - (\sum a)^2}\sqrt{z(\sum b^2) - (\sum b)^2}} \quad (11)$$

Where *n* is the total number of cumulative infiltrations, *pi* is the mean simulated cumulative infiltration, and *m*i is the mean observed cumulative infiltration. The RMSE provides an overall idea of the dispersion between measured and predicted cumulative infiltration (Vand *et al*., 2018; Amami *et al*., 2021).

Corresponding author's e-mail address: johnmusa@futminna.edu.ng

2.4.4 Single Factor Analysis of Variance (ANOVA)

The single factor ANOVA is employed to ascertain if there are statistically significant differences between the means of two or more independent groups. Most importantly, it tests the null hypothesis (H_0)

$$H_0: \mu_1 = \mu_2 = \mu_3 = \mu_4 \ldots\ldots\ldots = \mu_k \quad (12)$$

Where μ is the group mean, and k is the number of groups. If the one-way ANOVA returns a statistically significant result in an Excel sheet, single-factor ANOVA will provide the value of F, F-critical and P values.

3.0 Results

Table 1 presents the soil textural classification of the study location with a slight difference between the sample collection depths. This is in accordance with the study by DeArmond *et al.* (2019). The soil samples collected from the fifteen plots within the study area at 0–30 cm and 30–60 cm indicated that the average soil moisture and bulk density ranged from 7.14 to 17.07 % and 1.40 to 1.80 g/cm^3, respectively.

Table 1: Physical properties of soil samples collected from the study location

Samples	Soil depth (cm)	% Sand	% Silt	% Clay	Textural class	Moisture content (%)	Bulk density (g/cm^3)
A	0 - 30	71.00	13.66	15.34	Sandy loam	13.51	1.56
	30 - 60	32.15	53.63	14.22	Silty Loam	14.13	1.26
B	0 - 30	76.10	7.20	16.70	Sandy loam	16.64	1.53
	30 - 60	21.65	38.64	39.71	Clay loam	13.85	1.61
C	0 - 30	72.40	14.60	13.00	Sandy loam	12.35	1.20
	30 - 60	77.21	15.39	7.40	Loamy sand	8.72	1.80
D	0 - 30	83.10	10.25	6.65	Loamy sand	8.43	1.49
	30 - 60	81.25	7.56	11.19	Loamy sand	9.54	1.30
E	0 - 30	78.12	7.73	14.15	Sandy loam	12.33	1.58
	30 - 60	58.12	23.44	18.44	Sandy loam	10.37	1.35
F	0 - 30	66.76	18.20	15.04	Sandy loam	7.93	1.72
	30 - 60	87.10	2.53	10.37	Loamy sand	6.35	1.52
G	0 - 30	71.16	14.22	14.62	Sandy loam	15.77	1.97
	30 - 60	25.18	36.57	38.25	Clay loam	11.10	1.47
H	0 - 30	63.15	23.70	13.15	Sandy loam	13.48	1.68
	30 - 60	60.31	22.30	17.57	Sandy loam	12.23	1.60
I	0 - 30	80.25	15.32	4.43	Loamy sand	11.65	1.78
	30 - 60	35.23	31.95	32.82	Clay loam	14.66	1.46
J	0 - 30	82.28	9.36	8.36	Loamy sand	12.73	1.62
	30 - 60	50.42	21.03	28.55	Sandy clay loam	11.47	1.28
K	0 - 30	65.90	8.93	25.17	Sandy clay loam	17.26	1.69

Corresponding author's e-mail address: johnmusa@futminna.edu.ng

	30 - 60	11.50	49.40	39.10	Silty clay	16.87	1.27
L	0 - 30	79.55	6.36	14.09	Sandy loam	12.29	1.42
	30 - 60	25.15	60.75	14.10	Silty Loam	14.64	1.72
M	0 - 30	71.40	16.16	12.44	Sandy loam	15.46	1.25
	30 - 60	35.51	30.83	33.66	Clay loam	11.14	1.62
N	0 - 30	80.11	5.74	14.15	Sandy loam	12.84	1.95
	30 - 60	65.20	4.28	30.52	Sandy clay loam	12.08	1.65
O	0 - 30	68.52	13.38	18.10	Sandy Loam	13.99	1.23
	30 - 60	72.33	3.25	24.15	Sandy clay loam	11.49	1.60

3.1 Infiltration Curves

The cumulative infiltration for 15 plots is presented in Figure 1 (a to o). The cumulative infiltration graph of the observed and predicted (Kostiakov, Philip, Modified Kostiakov, and SCS) was plotted against the elapsed time.

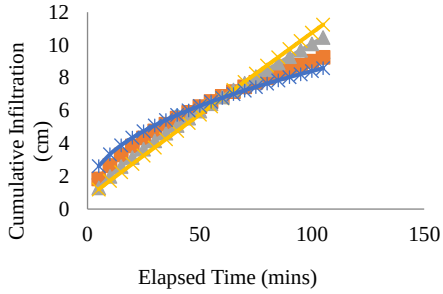

a.

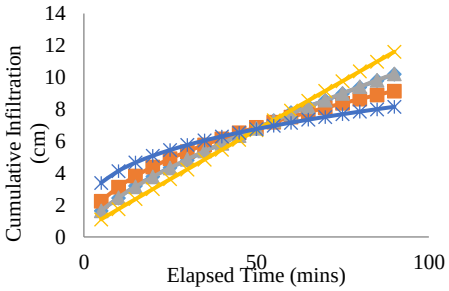

b.

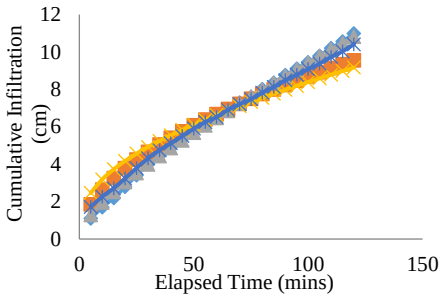

c.

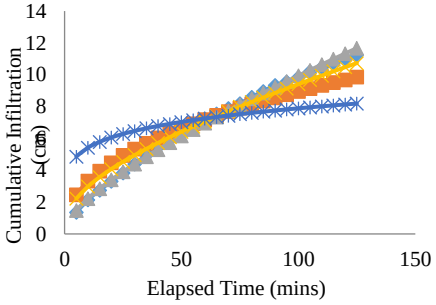

d.

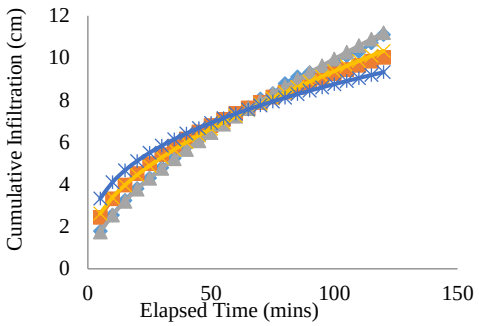
Cumulative Infiltration (cm)
Elapsed Time (mins)

e.

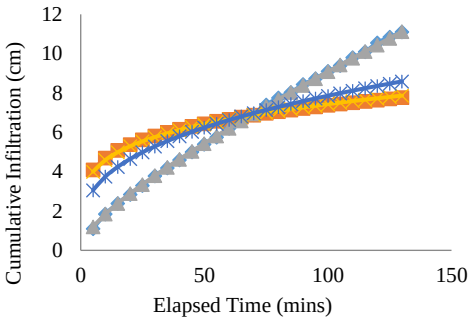
Cumulative Infiltration (cm)
Elapsed Time (mins)

f.

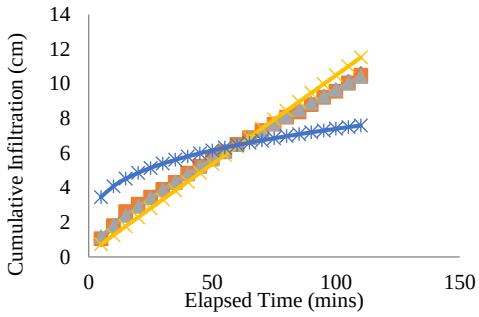
Cumulative Infiltration (cm)
Elapsed Time (mins)

g.

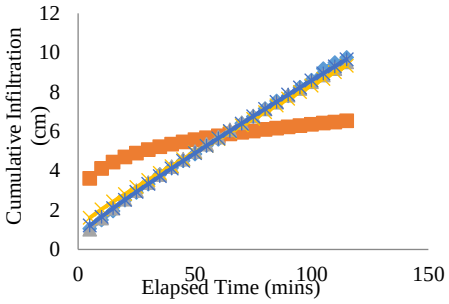
Cumulative Infiltration (cm)
Elapsed Time (mins)

h.

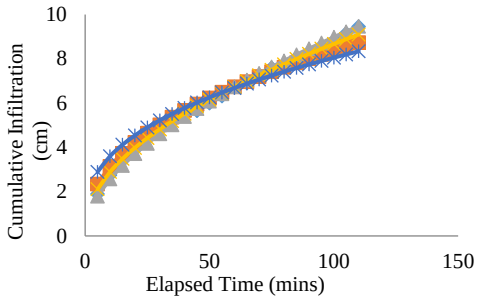
Cumulative Infiltration (cm)
Elapsed Time (mins)

i.

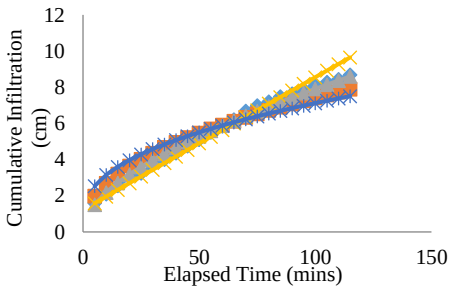
Cumulative Infiltration (cm)
Elapsed Time (mins)

j.

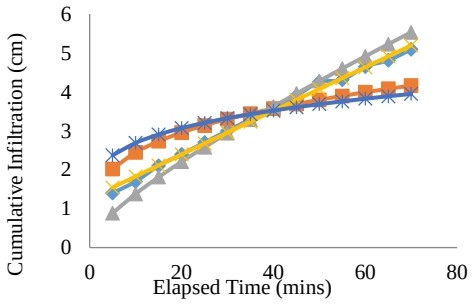
Cumulative Infiltration (cm)
Elapsed Time (mins)

k.

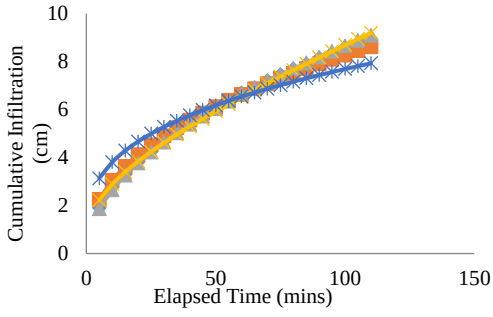
Cumulative Infiltration (cm)
Elapsed Time (mins)

l.

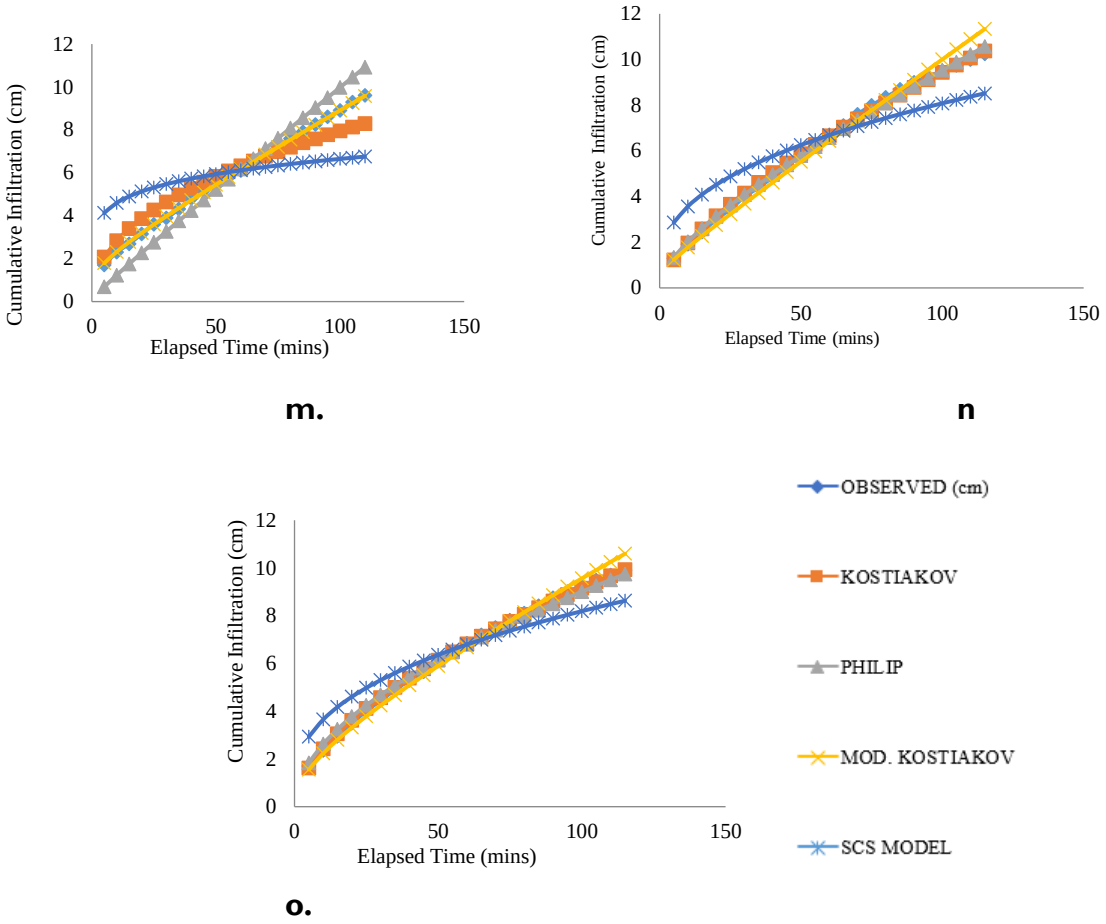

Figure 1: Cumulative infiltration for the observed and prediction models

Table 2 presents field data for the various infiltration rate models considered for this study, while Tables 3 and 4 present the average values of the performance evaluation parameters of infiltration models and the average results of the single factor ANOVA test for different infiltration models

Table 2: Parameters of the selected infiltration models for each of the fifteen plots

Sampled Plot	Kostiakov's		Philip		Modified Kostiakov			SCS model	
	K	**a**	**S**	**A**	**K**	**A**	**f_0**	**a**	**b**
A	0.790	0.529	0.458	0.055	0.652	0.057	0.099	0.908	0.464
B	1.020	0.488	0.631	0.047	0.429	0.089	0.122	1.527	0.352
C	0.801	0.518	0.468	0.047	1.366	0.344	0.017	0.932	0.978
D	1.235	0.430	0.571	0.042	1.130	0.373	0.031	3.103	0.183
E	1.193	0.445	0.719	0.028	1.464	0.327	0.028	1.443	0.373
F	2.987	0.196	0.432	0.048	2.279	0.236	0.667	1.302	0.370
G	1.047	0.976	0.399	0.057	0.195	0.072	0.102	1.708	0.297
H	2.665	0.189	0.343	0.051	1.069	0.113	0.065	0.118	0.913
I	1.178	0.426	0.775	0.012	1.012	0.440	0.010	1.145	0.404

Corresponding author's e-mail address: johnmusa@futminna.edu.ng

J	0.973	0.441	0.646	0.014	1.198	0.012	0.073	0.935	0.418
K	1.302	0.274	0.300	0.043	1.251	0.007	0.056	1.115	0.252
L	1.120	0.434	0.826	0.004	1.254	0.305	0.036	1.383	0.352
M	1.008	0.448	0.109	0.089	1.078	0.197	0.062	2.557	0.183
N	0.410	0.681	0.495	0.046	0.599	0.181	0.086	1.116	0.410
O	0.638	0.578	0.799	0.010	0.673	0.407	0.052	1.165	0.404

Table 3: Average values of the performance evaluation parameters of infiltration models

Model	RMSE	R^2	CC
Kostiakov	0.6124	0.9849	0.992
Philip	0.2116	0.9977	0.999
Modified Kostiakov	0.5262	0.9911	0.996
SCS	0.9815	0.9821	0.991

Table 4: Average results of the single factor ANOVA test for different infiltration models

Approaches	F	P-value	f-critical
Kostiakov Model	0.009249	0.948290	4.090291
Philip Model	0.00077	0.988993	4.033874
Mod. Kostiakov Model	0.003814	0.968504	4.090291
SCS model	0.020821	0.900067	4.090291

4.0 Discussion

The quantity of water plants needed from sowing to harvest is the available soil water/moisture content (Musa *et al.,* 2020). Soil moisture content is a critical factor influencing various soil functions and processes. This function includes plant growth, physical and chemical properties, soil biological activity, erosion, and runoff. Managing soil moisture content is critical for promoting sustainable agriculture. The result obtained is similar to the works of Uloma *et al.* (2014) in a different location where moisture content ranged between 7.1% to 17.5%.

Furthermore, it was discovered that a constant infiltration rate was achieved within a minimal time at location K, which had a high moisture content. The longer it takes for the soil to establish a stable infiltration rate, the lower the infiltration rate and the higher the initial soil moisture content. This is connected to the texture of the soils and the level of compaction of the soils in the study areas. The rate at which water enters the soil also increases with soil dryness (Musa and Adeoye, 2010). In other circumstances, the cumulative infiltration volume decreases as the initial soil moisture content rises, according to Qing *et al.* (2020). The high moisture-holding ability of clay, which was discovered to be expected at this soil layer, is thought to be the cause of the detected discrepancy. As indicated by Umaru *et al.* (2021), the highest value of the soil's average moisture content may be beneficial for crops that constantly require water, which may thrive in waterlogged conditions. The results contradict those of Musa *et al.* (2019), who investigated the effect of water stress on the yield of selected vegetable crops in Nigeria's Southern Guinea Savannah Ecological Zone. This can be attributed to the study area's seasonal

Corresponding author's e-mail address: johnmusa@futminna.edu.ng

variation, soil structure, texture, and climate change (Umaru *et al.,* 2021). However, the locations are contiguous within the same study environment. According to Musa and Adeoye (2010), initial movement and the overall amount of infiltration were thought to be influenced by the initial soil moisture content at any given time, both of which decreased as the soil moisture content increased. According to several studies, sandy soil has a higher infiltration rate than clay soil under the same circumstances (Runbin, 2011; Igbadun *et al.,* 2016). Musa *et al.* (2017) assert that all water will enter if the water at the soil surface exceeds the infiltration capacity. This is related to plot F's low soil moisture content reading.

Bulk density is a sign of the health and compaction rate of the soil. This is also believed to affect the depth or limitations of plant roots, soil water holding capacity, plant nutrition availability, soil porosity, soil microbe activity, and nutrient availability, all of which have an impact on soil productivity (Arévalo-Gardini *et al.,* 2015). It was observed that plot N had the highest value of the soil bulk density, ranging from 1.40 to 1.80 g/cm^3. The bulk density values observed in this study are similar to those discovered by Igboekwe and Adindu (2014) in an entirely separate region, with this finding ranging from 1.40 to 1.80 g/cm^3. A rise in infiltration capacity has been seen to be closely related to a fall in bulk density. The high percentage of clay content, the potential proximity of underlying rocks to the soil surface, and mechanical impedance may all have contributed to plot N's high bulk density.

The difference in bulk density measurements may be related to prevailing variables such as the soil's degree of compaction in the study area, the volume of the core ring, and the depth at which the soil samples were taken. Bulk density rises with the degree of compaction, which may be caused by the impact of farming techniques and rainfall events on the topsoil, according to Musa and Adeoye (2010). Thus, soil compaction has been linked to flooding, as Grzesiak et al. (2016) and Ferreira et al. (2018) documented.

This study showed that sandy soil was most predominant, as this demonstrates that the saturated hydraulic conductivity of a particular soil is significantly determined by the actual amount of sand in that soil sample (Musa *et al.,* 2020, 2021). Plot D had the highest percentage of sand compared to other study locations. Each soil sample from plots A to O holds a different amount of sand, ranging from 11.50% at 0 to 30 cm depth to 83.10% at 30 to 60 cm depth. Similarly, the silt content of plot L is higher than that of the other samples, while the clay content of plots K and B is higher than that of the other samples at both depths. Plots J, N, and 0 at a depth level of 30-60 cm and plot K at a depth level of 0-30 cm, respectively, showed the highest values of sandy clay loam, which is easily detached but difficult to transport (Bonilla and Johnson, 2012; Mirzaee *et al.,* 2017) while the lowest concentrations of silt loam and silt clay were found at plots A and L, each at a depth of 30 to 60 cm, and plot K, also at a depth of 30 to 60 cm respectively. The study area reveals some degree of variation in the percentages of sand, silt, and clay in the various soil samples that were collected, which is comparable to the works of Okon *et al.* (2017) and Deb *et al.* (2019) for the differences in physicochemical properties of soils under oil palm plantations of different ages in Ohaji/Egbema, Imo State, and Variability of soil physicochemical

properties at different agroecological zones of Himalayan region: Sikkim, India respectively. At a depth of 0 to 30 cm, the highest sand value was 83.10%. According to Girei *et al.* (2016), higher soil resistance to continuous cultivation may be the cause of the increased sand fraction in plot D. The data collected in the field showed that there are low silt/clay soil ratios, which may suggest that the study region has not been effectively used for agriculture, resulting in a low level of erosion activities. The findings of the study conducted by Afolabi *et al.* (2014) on the Evaluation of Some Soils of Minna Southern Guinea Savanna of Nigeria for Arable Crop Production within the Permanent Site Irrigation Farm of the Federal University of Technology, Minna is invalidated by the current findings. This can be ascribed to the spatial heterogeneity of the research region and additional physical characteristics of the soil, such as the soil structure, porosity, and moisture content, which may also impact the infiltration process (Yan *et al.,* 2013).

Infiltration tests were conducted on-site to address the regional heterogeneity of the infiltration rate. As a result, the study area's initial and final infiltration rates vary from 1080 to 1176 cm/h. Results from Figures 1 (a to o) show that the infiltration data for Plots K and B reached field capacity more quickly and had the lowest infiltration readings. This can be attributed to the plots' high initial soil moisture content values and high bulk densities from soil compaction, as expressed in Table 1. Low values of the infiltration characteristics point to potentially excessive runoff (erosion) on such topo-sequences or slopes (Oku and Aiyelari, 2011). Another explanation for the poor infiltration rate in the study could be the spatial diversity of soil parameters within the field (Bui *et al.,* 2019). It was observed that Plots F, D, C, and E took longer to be saturated than other plots due to the high bulk density noted in the plots. Low bulk density, however, may cause a high infiltration rate, as seen in the C, D, E, J, M, and O plots. In addition, the soil particles at plots F, G, I, H, L, and N were wetter than those at the other spots, which caused them to permeate water more slowly than the other points. Therefore, the soil aggregates' shape, size, and stability may impact the infiltration rate.

Contrary to the findings of (Ieke *et al.,* 2013), coarse-grained sandy soils are known to contain vast gaps between each grain, which allows water to penetrate quickly. Until a steady state is reached, soil infiltration rates gradually decrease. Several variables affect infiltration, such as soil texture, structure, initial soil water content, pore size, soil metric potential, and vegetation (Al-Janobi *et al*., 2010). This tendency is also evident in the cumulative infiltration presented in Figure 1.

The rainfall-runoff mechanism must be understood using data on water infiltration for various soil types. Table 2 describes the infiltration equation's parameters, and Figure 1 (a to o) displays graphs of the calculated infiltration rate. The values of the empirical constant 'K' and the infiltration decay constants' a' for Kostikov's infiltration model were calculated to be in the range of 0.4099 to 2.9866 and 0.1888 to 0.9763, respectively. The values of the infiltration decay constant 'a' were consistent with the infiltration hypothesis, which stated that the values should always be positive and less than unity. According to reports from Ogbe *et al.* (2011) and Farid *et al.* (2019), most of these parameters' values fall between 0.2 and 0.9. In addition, the sorptivity

(*S*) values were found in the range of 0.1087 to 0.8264 cm/min, and the conductivity constant (*A*) values ranged between 0.0038 and 0.0889 cm/min for all fifteen plots of Philip's infiltration model. The *S*-estimated values and those provided by Vand *et al.* (2018) agreed with most of the findings in the study area. Similar to this, the values of the parameters of the Modified Kostiakov's model, such as *k*, were determined to range between 0.0069 and 0.4400, and the infiltration decay constants *a* and f_0 were determined to range between 0.0099 and 0.6671. Finally, the values for the SCS model's infiltration parameters, such as *a*, were obtained in the range of 0.9353 to 3.1025 and those for *b*, between 0.1825 and 0.9777. Although the values of the model's infiltration parameters have no physical significance, they reflect the influence of the soil's physical characteristics on infiltration, the state of the surface, and the soil's moisture content (Ogbe *et al.,* 2011). Farid *et al.* (2019) reported using the Coefficient of Determination (R^2) as a metric to compare the infiltration models. In particular, the Absolute Mean Difference (AMD) and R^2 were employed to compare Kostikov's and Philip's models. Haghighi *et al.* (2010) used the R^2 and root mean square error (RMSE) metrics to choose the optimal model for infiltration data. Igbadun and Idris (2007) employed the efficiency coefficient to assess the infiltration model's applicability. The estimated average Coefficient of Correlation (CC) values were 0.992, 0.999, 0.996, 0.991; the estimated average R^2 values were 0.9849, 0.9977, 0.9911, 0.9821 (Table 3); and the estimated average Root Mean Square Error (RMSE) values were 0.6124, 0.2116, 0.5262, and 0.9815 cm/min. The infiltration rate highly depends on soil texture (Haghighi *et al.,* 2010), and the result is consistent with the findings of Thomas *et al.* (2020). They evaluated six infiltration equations on homogeneous coarse-textured soils. They also found that Philip's model provided an excellent representation of the infiltration. At the same time, Kostiakov, modified Kostiakov, Green Apmt, and Holtan-Overton performed in that order, as Igbadun et al. (2016) suggested. Oku and Aiyelari (2011) likewise anticipated cumulative infiltration beneath the Inceptisols in the humid forest zones. The outcome demonstrated that Philip's model was more appropriate than the Kostiakov model. However, the findings of this study are in contrast to those of Igbadun *et al.* (2007), who reported that the Kostiakov model related closely to the measured data than Philip's model for a hydromorphic soil at Samura, Nigeria, and the findings of Musa and Adeoye, (2010) who studied the adaptability of infiltration equations to soils of the permanent site farm of the Federal university of technology, Minna, in the guinea savannah zone of Nigeria and found that the Kostiakov model fit the data better than the Horton and Philip models. This can be attributed to several elements, including spatial variability, rainfall patterns, vegetation types, soil water content, soil characteristics of the study area, and the fact that the previous study was carried out in an undeveloped area with a rural setting. In contrast, the current study was carried out in an urban setting.

Table 4 shows that the F-F-statistic for all models is less than the P-value and f-critical. If the F-statistic is less than the p-value and the f-critical value in a model, it suggests no significant difference between the means of the groups being compared. This conclusion can be drawn because the F-statistic tests whether the variability between groups is more significant than within groups. A low F-value indicates that the variability between groups is not much larger than the

variability within groups, which suggests that there is no significant difference between the means of the groups being compared. Therefore, when the F-statistic is less than the f-critical value, and the p-value is more significant than the alpha level (typically 0.05), it is appropriate to fail to reject the null hypothesis and conclude that there is not statistically significant difference between the group means.

5.0 Conclusion

Most of the soils in the study area were sandy loam, which may be the cause of the relatively low infiltration rate seen in the area. Thus, it can be deduced that bulk density and soil texture have a more significant impact on infiltration rate than moisture content, which caused the infiltration of the study area to be low; hence, water logging at some points.

This study concluded that Philip's model was substantially closer to the observed data when the field and predicted infiltration rates were compared. Philip's model outperformed the other four infiltration models to estimate infiltration rate in specific land use and soil parameter models. The model offered the lowest values, which led to the conclusion that it accurately captured the infiltration rate based on the mean values of RMSE. Therefore, it is concluded that the Philip model can be utilised more effectively to simulate cumulative infiltration to generate infiltration data artificially where there is no actual infiltration data for the studied area.

Reference

Afolabi, SG., Adeboye, MKA., Lawal, BA., Adekanmbi, AA., Yusuf, AA. and Tsado, PA. 2014. Evaluation of Some Soils of Minna Southern Guinea Savanna of Nigeria for Arable Crop Production. Nigerian Journal of Agriculture, Food and Environment, 10(4): 6-9.

Al-Janobi, AA., Aboukarima, AM. And Ahmed, KA. 2010. Modelling Water Infiltration Rate under Conventional Tillage Systems on a Clay Soil Using Artificial Neural Networks. Australian Journal of Basic and Applied Sciences, 4(8): 3869-3879.

Angelaki, A., Sakellariou-Makrantonaki, M. and Tzimopoulos, C. 2013. Theoretical and experimental research of cumulative infiltration. Transport Porous Media, 100(2): 247–257.

Barros, CAP., Minella, JPG., Tassi, R., Dalbianco, L. and Ottonelli, AS. 2014. Estimation of soil water infiltration at the catchment scale. Revista Brasileira de Ciência do Solo, 38: 557-564. http://dx.doi.org/10.1590/S0100-06832014000200020

Bonilla, CA. and Johnson, OI. 2012. Soil erodibility mapping and its correlation with soil properties in Central Chile. Geoderma, 189: 116-123.

Deb, P., Debnath, P., Denis, AF. and Lepcha, OT. 2019. Variability of soil physicochemical properties at different agroecological zones of Himalayan region: Sikkim, India. Environment, Development and Sustainability, 21(5): 2321-2339>

DeArmond, D., Emmert, F., Lima, AJN. and Higuchi, N. 2019. Impacts of soil compaction persist 30 years after logging operations in the Amazon Basin. Soil and Tillage Research, 189: 207-216.

Farid, HU., Mahmood-Khan, Z., Ahmad, I., Shakoor, A., Anjum, MN., Iqbal, MM., Mubeen, M. and Asghar, M. 2019. Estimation of infiltration models parameters and their comparison to simulate the on-site soil infiltration characteristics. International Journal of Agricultural and Biological Engineering, 12(3): 84–91.

Ferreira, CS., Walsh, RP. and Ferreira, AJ. 2018. Degradation in urban areas. Current Opinion in Environmental Science and Health, 5: 19-25.

Girei, AH., Abdulkadir, A. and Abdu, N. 2016. Goodness of fit of three infiltration models of a soil under long-term trial in Samaru, Northern Guinea Savanna of Nigeria. Journal of Soil Science and Environmental Management, 7(5): 64-72. DOI:10.5897/JSSEM2015.0525

Grzesiak, MT., Janowiak, F., Szczyrek, P., Kaczanowska, K., Ostrowska, A., Rut, G. and Grzesiak, S. 2016. Impact of soil compaction stress combined with drought or waterlogging on physiological and biochemical markers in two maise hybrids. ActaPhysiologiaePlantarum, 38(5): 109.

Haghighi, F., Gorji, M., Shorafa, M., Sarmadian, F. and Mohammadi, MH. 2010. Evaluation of some infiltration models and hydraulic parameters. Spanish Journal of Agricultural Research, 8 (1): 210-217, 10.5424/sjar/2010081-1160

Hillel, D. 1982 Introduction to Soil Physics. Academic Press Inc., New York, USA.

Ieke, W.A., Prijino, S. and Soemarno, P. 2013. Assessment of Infiltration Rate under Different Dryland Types in Unter-Iwes Subdistrict Sumbawa Besar, Indonesia. Journal of Natural Sciences Research, 3, (10): 71-76.

Igbadun, HE. and Idris, UD. 2007. Performance Evaluation of Infiltration Models in a Hydromorphic Soil. Nigerian Journal of Soil and Environmental Research, 7: 53-59. https://doi.org/10.4314/njser.v7i1.28418

Igbadun, H., Othman, M. and Ajayi, A. 2016. Performance of Selected Water Infiltration Models in Sandy Clay Loam Soil in Samaru Zaria. Global Journal of Research in Engineering: Journal of General Engineering, 16, 8-14.

Igboekwe, MU. and Adindu, RU. 2014. Use of Kostiakov's Infiltration Model on Michael Okpara University of Agriculture, Umudike Soils, Southeastern, Nigeria. Journal of Water Resource and Protection, 6: 888-894

Jury, WA. and Stolzy, LH. 2018. Soil Physics. Handbook of Soils and Climate in Agriculture, Edited by Victor J. Kilmer, 131-158. CRC Press, Boca Raton, Florida, USA.

Kostiakov, AN. 1932. On the dynamics of the coefficient of water percolation in soils and on the necessity for studying it from a dynamic point of view for purposes of amelioration. Society of Soil Science, 14, 17-21

Lal, R. 2018. Land Use and Soil Management Effects on Soil Organic Carbon Dynamics on Alfisols in Western Nigeria. In Soil processes and the carbon cycle 123-140. CRC Press, CRC Press, Boca Raton, Florida, USA.

Mirzaee, S., Ghorbani-Dashtaki, S., Mohammadi, J., Asadzadeh, F. and Kerry, R. 2017. Modelling WEPP erodibility parameters in calcareous soils in northwest Iran. Ecological Indicators, 74: 302-310.

Mirzaee, S., Zolfaghari, AA., Gorji, M., Dyck, M., and Ghorbani DS. 2014. Evaluation of infiltration models with different numbers of fitting parameters in different soil texture classes. Archives of Agronomy and Soil Science, 60(5): 681-693.

Musa, JJ. and Adeoye, PA. 2010. Adaptability of infiltration equations to the soils of the Permanent Site Farm of the Federal University of Technology, Minna, in the Guinea savannah zone of Nigeria. Assumption University Journal of Technology, 14(2): 147-155.

Musa, JJ., Akpoebidimiyen, OE., Adewumi, JK., Eze, PC., Adesiji, R. and Gupa, Y. U. 2020. Influence of Soil Bulk Density and Porosity on Soil Hydraulic Conductivities for Selected Land Management Practice in Northcentral Nigeria. International Journal of Agricultural and Environmental Sciences, 5(1): 1-7.

Musa, JJ., Akpoebidimiyen, OE., Dada, POO., Adewumi, JK. and Gupa, YU. 2021. Effect of Land Management on Soil Hydraulic Conductivity in Gidan Kwano, Niger State, Nigeria. Open Journal of Forestry, 11: 108-116. https://doi.org/10.4236/ojf.2021.112008

Musa, JJ., Anijofor, SC., Obasa, P. and Avwevuruvwe, JJ. 2017. Effects of soil physical properties on erodibility and infiltration parameters of selected areas in Gidan kwano. Nigerian Journal of Technological Research. 12(1):17-26. DOI: http://dx.doi.org/10.4314/njtr.v12i1.8

Musa, J., Adewumi, J., Otuaro, E. and Musa, M. 2019. Effect of Water Stress on the Yield of Selected Vegetable Crops in the Southern Guinea Savannah Ecological Zone of Nigeria. Open Access Library Journal, 6: 1-12. doi: 10.4236/oalib.1105938.

Musa, J.J. and Egharevba, N.A. 2009. Soil Grouping of the Federal University of Technology, Minna, Main Campus Farm Using Infiltration Rate. Assumption Journal of Technology, 13 (1), 19-28.

Ogbe, VB., Jayeoba, OJ. and Ode, SO. 2011. Comparison of four soil infiltration models on a sandy soil in Lafia, Southern Guinea Savanna Zone of Nigeria. Production Agriculture and Technology, 7(2): 116–126.

Okon, MA., Nwachukwu, MN. and Osujieke, DN. 2017. Differences in physicochemical properties of soils under oil palm plantations of different ages in Ohaji/Egbema, Imo State. International Journal of Research, 4(1): 1-7

Oku, E. and Aiyelari, A. 2011. Predictability of Philip and Kostiakov Infiltration Model under Inceptisols in the Humid Forest Zone, Nigeria. Kasetsart Journal (Natural Science), 45: 594-602.

Panagos, P., Meusburger, K., Ballabio, C., Borrelli, P. and Alewell, C. 2014. Soil Erodibility in Europe: A high-resolution dataset based on LUCAS. Science of the Total Environment, 4 (7): 189 - 200.

Philips, JR. 1957. The theory of infiltration: The infiltration equation and its solution. Soil Science, 83 (5): 345-358, DOI: 10.1097/00010694-195705000-00002.

Qing, X., Haojie, H., Jinran, X., Caixia, Z., Zhiliang Z., Huiqiang, H., and Qin, Z. 2020. Research Progress of Soil Water Infiltration. E3S Web of Conferences, 189: 01006. https://doi.org/10.1051/e3sconf/202018901006

Runnbin, D., Clifford, B. and Fedler, JB. 2011. Field Evaluation of Infiltration Models in lawn Soils. Irrigation Science, 29: 379-389.

Sihag, P., Tiwari, NK. and Ranjan, S. 2017. Estimation and intercomparison of infiltration models. Water Science, 31(1): 34-43. DOI: 10.1016/j.wsj.2017.03.001.

Sollins, P. and Gregg, JW. 2017. Soil organic matter accumulation in relation to changing soil volume, mass, and structure: Concepts and calculations. Geoderma, 301: 60-71

Thomas, AD., Ofosu, AE., Emmanuel, A., De-Graft, AJ., Ayine, AG., Asare, A. and Alexander, A. 2020. Comparison and Estimation of Four Infiltration Models. Open Journal of Soil Science, 10: 45-57. https://doi.org/10.4236/ojss.2020.102003

Uloma, AR., Samuel, AC. and Kingsley, IK. 2014. Estimation of Kostiakov's infiltration model parameters of some sandy loam soils of Ikwuano–Umuahia, Nigeria. Open Transactions on Geosciences, 1 (1): 34-38,

Umaru, AB., Tya, TSK., Musa, MM. and Vanke, I. 2021. Effects of Some Soil Physical Properties on Infiltration Rate at Phase 2b of Lake Geriyo Irrigation Project, Yola, Nigeria. Nigeria Journal of Engineering Science and Technology Research, 7 (1): 74-83.

Valiantzas, JD. 2010. New linearised two-parameter infiltration equation for direct determination of conductivity and sorptivity. Journal of Hydrology 384(1–2):1–13

Vand, SA., Sihag, P., Sing, B. and Zand, M. 2018. Comparative evaluation infiltration models. KSCE Journal of Civil Engineering, 22 (10): 4173-4184

Yan, YH., Zheng, JY. and Zhang, C. 2013. Impact of biochar addition into typical soils on field capacity in Loess Plateau. Journal of Soil and Water Conservation, 27(4): 120–124